Resonance Raman Evidence for a Novel Charge Relay Activation Mechanism of the CO-Dependent Heme Protein Transcription Factor CooA[†]

Kathleen M. Vogel and Thomas G. Spiro*

Department of Chemistry, Princeton University, Princeton, New Jersey 08544

Daniel Shelver, Marc V. Thorsteinsson, and Gary P. Roberts

Department of Bacteriology, University of Wisconsin, Madison, Wisconsin 53706

Received October 5, 1998; Revised Manuscript Received December 28, 1998

ABSTRACT: Resonance Raman spectra of the CO-responsive transcription factor CooA from *Rhodospirillum rubrum* provides evidence on the nature of heme ligation and its CO activation mechanism. The Fe(III) form gives standard low-spin heme spectrum, while the Fe(II) form is low spin for wild-type (WT) CooA and mixed spin for a CooA variant, H77Y, with an His77Tyr substitution. The Fe(II) porphyrin skeletal mode ν_{11} is at a value (1541 cm^{-1}) indicative of a neutral donor ligand for the H77Y variant but is at an unusually depressed frequency (1529 cm^{-1}) for the WT protein, indicating a strongly donating ligand. This ligand is proposed to be His77 imidazolate, formed by proton transfer to a nearby acceptor. The WT CO adduct has FeCO and CO stretching frequencies that indicate a neutral trans ligand and negative polarity in the CO binding pocket, while the CO adduct of His77Tyr has both 6- and 5-coordinate signals and a nonpolar CO environment. Photolysis of the WT CO adduct by the Raman laser produced a low-spin product at steady state, indicating fast recombination of the displaced ligand. These data suggest a novel YH- - -His^- charge relay mechanism for CooA activation by CO. In this mechanism, His77 is reprotonated upon ligand displacement by CO; CO displaces either His77 or the trans ligand, X. The resulting charge on Y^- may induce the protein conformation change required for site-selective DNA binding.

In addition to their multifarious roles in electron transfer and in oxygen binding and activation, heme proteins have recently emerged as important signal transducers in biology. The heme prosthetic group binds CO, NO,[1] and O_2 strongly and is therefore an effective sensor for these ubiquitous small molecules. Heme-containing proteins have evolved ways of coupling these binding events to enzyme activation (e.g., the NO receptor, guanylyl cyclase) or gene regulation (e.g., the O_2 or CO sensors FixL and CooA) (*1*−*6*). The mechanisms of this coupling and the basis of specificity are important themes for current research. Since the heme group has two axial sites for ligation, the nature and dynamics of the endogenous ligands in these proteins are likely to be key factors in the mechanisms. It is already known, for example, that a proximal ligand is displaced when NO, but not CO, binds to guanylyl cyclase, and this displacement is likely to initiate a conformation change that activates the enzymatic region of the protein (*7*−*11*).

The CooA transcription factor from *Rhodospirillum rubrum* responds to CO by activating two operons that encode a CO-oxidizing system (*12*, *13*). It is a dimeric heme-containing protein that binds CO in the Fe(II) form (*6*). CO binding induces CooA to bind DNA in a site-specific manner (*6*, *14*). By analogy with CRP, a CooA homologue (*15*), this ability to bind DNA probably reflects a conformational change in CooA upon CO binding (*16*). The heme of WT CooA is 6-coordinate and low spin in the Fe(III) form (*6*), and its EPR spectrum shows that one of the ligands is thiolate (*6*, *17*, *18*). Site-directed mutagenesis and analysis of CooA variants have implicated Cys75 as the thiolate ligand (*19*). The Fe(II) form is also 6-coordinate, implying that CO must displace an endogenous ligand (*6*, *18*). Since this displacement may provide the trigger for conformational changes leading to high-affinity DNA binding, we sought to investigate the nature of this displacement, using resonance Raman spectroscopy. This technique provides structural information from the frequencies and intensities of vibrational modes involving the heme and its ligands. In combination with mutational, functional, and other spectroscopic analyses (*17*, *19*), our results strongly suggest a novel charge relay mechanism for CO-dependent CooA activation.

METHODS

The CooA variants H77Y and C75S were obtained by site-directed and random local mutagenesis, respectively. Wild-type CooA and H77Y and C75S CooA were expressed in

[†] This work was supported by NIH Grants GM33576 (T.G.S.) and GM53228 (G.P.R.).

* To whom correspondence should be addressed.

[1] Abbreviations: CooA, CO oxidation activator; WT, wild type; RR, resonance Raman; CRP, cyclic AMP receptor protein; EPR, electron paramagnetic resonance; P450, cytochrome P450; heme, iron(II) protoporphyrin IX; NO, nitric oxide; LUMO, lowest unoccupied molecular orbital; Im, imidazole; cyt, cytochrome; sGC, soluble guanylyl cyclase; Mb, myoglobin; Hb, hemoglobin; FixL, *Rhizobium meliloti* O_2-sensing protein; Mops, 4-morpholinepropanesulfonic acid; OEP, octaethylporphyrin; TPP, tetraphenylporphyrin; BS, dibutyl sulfide; EPS, ethyl phenyl sulfide; MP8, microperoxidase 8.

10.1021/bi982375r CCC: $18.00
Published on Web 02/06/1999

Escherichia coli using the identical expression plasmid (*17*, *19*). Recombinant CooA was purified from *E. coli* by a procedure that is described in detail elsewhere (*19*). WT and H77Y CooA were purified by identical procedures to greater than 95% purity, as judged by densitometric scanning of Coomassie-stained SDS−PAGE gels. Due to the extreme oxygen lability of C75S CooA, this protein was anoxically purified to approximately 80% purity under reducing conditions (1 mM dithionite) and maintained under the identical conditions during analysis. DNase I footprinting was utilized to test the CO-dependent DNA-binding activity of purified CooA (*6*, *19*).

The purified CooA samples in 25 mM Mops/1 mM DTT (pH 7.4) were determined to contain varying concentrations of heme (60−360 μM), as determined by pyridine hemochrome (*20*). To prepare the samples for resonance Raman experiments, 300 μL of the protein was placed in a septum-sealed 0.5 mm o.d. NMR tube. The Fe(III)CooA was reduced by purging the protein sample with argon for 20 min, followed by anaerobic addition of 1.7 mM sodium dithionite solution. To obtain the CO adducts, separate NMR tubes containing Fe(II)CooA were reacted with 1 atm of either ^{12}CO (Matheson) or ^{13}CO gas (Cambridge Isotope Laboratories) for several minutes. Absorption spectra of Fe(III), Fe(II), and Fe(II)CO were obtained on a Hewlett-Packard 8452A diode array spectrophotometer to confirm the oxidation state and binding of CO.

Resonance Raman spectra were obtained with excitation wavelengths of 406.7, 413.1, 530.8, and 568.1 nm from a Kr^+ laser (Coherent Innova 100-K3) and 441.7 nm from a He−Cd (Liconix) laser in a backscattering sample geometry. Typically, low incident laser power of ~50 mW was focused with a cylindrical lens onto the sample. Except for the CO-photolyzed adduct, the protein samples were kept spinning throughout the laser illumination in order to reduce local heating and to minimize photodissociation of the bound ligands. The scattered light was collected and focused onto an Spex 1877 triple spectrograph equipped with a cooled, intensified diode array detector (Princeton Instruments, Inc.) or a Spex 1403 scanning double monochromator equipped with a photomultiplier tube, under computer control. Spectra were calibrated with toluene, indene, acetone, acetonitrile, DMSO-d_6, and CCl_4. For the depolarization measurements, a polarized scrambler was fixed in the scattering path. The parallel and perpendicular components of polarized light were calibrated by measuring CCl_4 under both conditions. All of the spectral data were imported to and processed with Labcalc software (Galactic Industries Corp.).

RESULTS

Fe(III) Form. The Fe(III) form of WT CooA has a standard low-spin absorption spectrum (424, 540, and 570 nm for the Soret, Q_1, and Q_0 bands), and the Soret-excited RR spectrum (Figure 1) is also standard (*21*). It is dominated by the ν_4 oxidation state marker band at 1375 cm^{-1}, and the higher frequency porphyrin skeletal modes are all at positions expected for low-spin Fe(III) heme (Table 1) (*22*). We note that the ν_{10} and ν_{11} positions are uncertain because of overlap with ν_{38} and with the vinyl C═C modes (*23*). In an effort to better understand the ligand structure of CooA, a variety of CooA variants have been constructed and analyzed (*19*). Of particular interest are variants that are altered at His77 and Cys75, and a H77Y variant has been studied in some detail. The high-frequency skeletal modes are 3−4 cm^{-1} lower for H77Y than for WT Fe(III) CooA, but the positions are all within the usual low-spin range (Figure 2). It has been established via EPR measurements that one of the Fe(III) ligands is thiolate (*17*), and site-directed mutagenesis implicates Cys75 as the ligating residue (*17*). RR spectroscopy provides no additional information on the Fe(III) ligation since the low-spin marker band positions are insensitive to the type of ligand in this oxidation state (Table 1) (*24*).

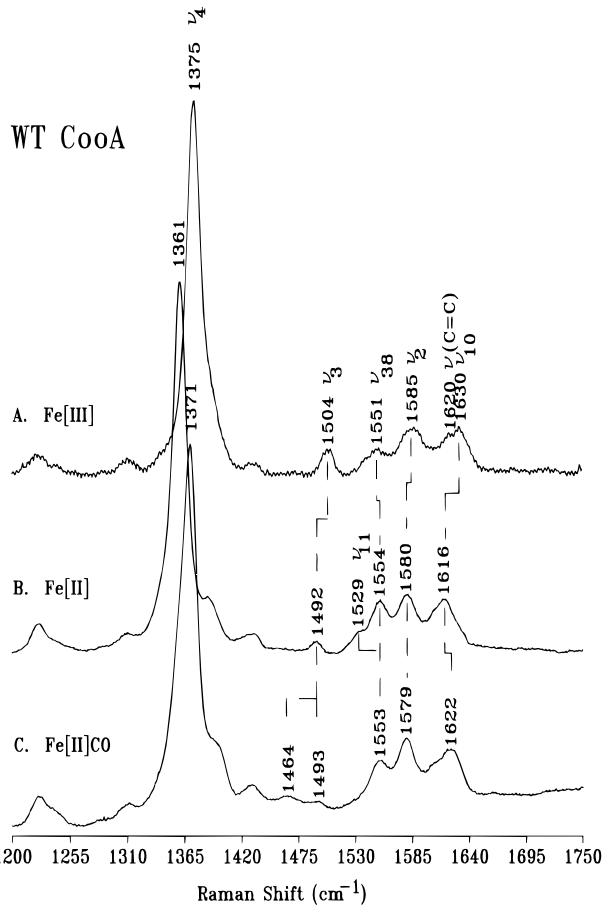

FIGURE 1: RR spectra in the porphyrin skeletal mode region for WT CooA (A) Fe(III), (B) Fe(II), and (C) Fe(II)CO, at pH 7.4. The porphyrin mode labeling is described in refs *25* and *52*. Excitation is at 413.1 nm.

Fe(II) Form: A Ligand Switch. RR spectra are more responsive to the nature of low-spin heme axial ligands in the Fe(II) than in the Fe(III) forms, because the Fe d_π orbitals are more extended in the lower oxidation state, and there is greater back-donation of d_π electrons into the porphyrin π^* orbitals. This results in lowered frequencies for certain porphyrin skeletal modes as a result of π bond weakening (*25*). When π acid ligands such as CO (see below) bind to the Fe(II) heme, they compete for the d_π electrons, and the π-sensitive porphyrin modes shift toward the values observed for Fe(III). The most sensitive of these π marker bands is ν_{11}, a rectangular distortion mode of the porphyrin, whose displacement is well matched to the lowest π^* orbital (LUMO) coefficients (*25*). This mode has the largest upshift upon CO binding or upon oxidation to Fe(III). It is also responsive to the donor strength of the axial ligands. A well-known example is its shift from 1547 to 1533 cm^{-1}, when

Table 1: RR Frequencies of Porphyrin Skeletal Modes for CooA and Select Heme Models (cm^{-1})[a]

protein/compd	ligation	ν_4	ν_3	ν_{11}	ν_2	ν_{10}	reference
			Fe(III)				
WT CooA	?	1375	1504		1585	1630	this work
H77Y	?	1372	1500		1581	1636	this work
			6-coordinate, low spin				
$PPIX(ImH)_2$	His/His	1373	1502	1562	1579	1640	*25*
cyt b_2	His/His	1374	1505		1579	1640	*53*
cyt P450(ImH)	Cys/His	1372	1500	1558	1585	1636	*54*
$OEP(BS)_2$	BS/BS	1374	1493	1561	1582	1628	this work
$OEP/(EPS)_2$	EPS/EPS	1374	1494		1583	1628	this work
			6-coordinate, high spin				
$Hb(F^-)$	His/F^-	1372	1480	1550	1564	1610	*25*
$PPIX(Me_2SO)_2$	$(Me_2SO)_2$	1370	1480	1545	1559	1610	*25*
			Fe(II)				
WT CooA	?	1361	1492	1529	1580	1616	this work
H77Y	?	1362	1472/1492	1541	1584	1605/1624	this work
C75S	?	1360	1491	1531	1581	1616	this work
			6-coordinate, low spin				
$PPIX(ImH)_2$	His/His	1359	1493	1539	1584	1617	*25*
cyt b_2	His/His	1361	1493	1537	1580	1620	*53*
$PPIX(ImH)(Im^-)$	ImH/Im^-	1359	1493	1526	1584	1614	*28*
$PPIX(Im^-)$	Im^-/Im^-	1358	1492	1517	1583	1613	*28*
Met80Cys cyt *c*	Cys/His	1360	1494	1537	1592	1625	*34*
$OEP(BS)_2$	BS/BS	1364	1462/1491	1550	1582	1621	this work
			5-coordinate, high spin				
PPIX(2-MeIm)	2-MeIm	1357	1471	1547	1562	1604	*25*
deoxy Hb	His	1358	1473	1546	1565	1607	*22*
$P450_{RLM3}$	Cys	1341	1463	1521	1564	1583	*24*

[a] Abbreviations: Im, imidazole; PPIX, protoporphyrin IX; PP, protoporphyrin IX dimethyl ester; cyt, cytochrome; OEP, octaethylporphyrin; Hb, hemoglobin; Met, methionine; Cys, cysteine; BS, dibutyl sulfide; EPS, ethyl phenyl sulfide; Me_2SO, dimethyl sulfoxide; 2-MeIm, 2-methylimidazole; RLM, rat liver microsomal. [b] Overlapped with ν_{38}. [c] Overlapped with $\nu_{(C=C)}$.

methionine is replaced by lysine, a stronger donor, as a ligand in Fe(II) cytochrome *c* (ν_{11} is somewhat higher in *c*-type than *b*-type cytochromes because of the saturation of the protoporphyrin vinyl groups) (*26*). Likewise ν_{11} shifts from 1539 to 1527 cm^{-1} upon deprotonation of the imidazole complex of microperoxidase or of bisimidazole Fe(II) protoporphyrin IX (*27*, *28*).

Because ν_{11} is weakly enhanced in Soret-resonant RR spectra and is overlapped with ν_{38} (Figure 1), we changed the excitation wavelength to the Q-band region, where the nontotally symmetric porphyrin modes are selectively enhanced (Figure 3) (*25*). Laser excitation at 530.8 nm, near resonance with Q_1, especially enhances A_{2g} symmetry modes, such as ν_{19}, which have most of their intensity in the perpendicularly polarized spectrum, while 568.1 nm excitation, near resonance with Q_0, especially enhances the B_{1g} symmetry modes, ν_{10} and ν_{11}, which have comparable intensity in perpendicular and parallel polarization (the expected ratio is 0.75) (*29*). These results clearly establish the ν_{11} frequency at 1529 cm^{-1}, implying ligation by a strong donor. The remaining band frequencies for Fe(II) CooA are at expected frequencies for low-spin Fe(II) heme (Table 1).

The H77Y variant is difficult to reduce (*6*); addition of dithionite produces a mixture of Fe(II) and Fe(III) forms. However, the Fe(III) contribution to the RR spectrum is readily subtracted by referencing the known spectrum to the amplitude of the well-separated ν_4 band (Figure 2). The resulting Fe(II) spectrum is a superposition of 6-coordinate low-spin and 5-coordinate high-spin contributions (Table 1). The high-spin contribution is clearly seen in the greatly downshifted ν_3 (1472 cm^{-1}) and ν_{10} (1605 cm^{-1}) bands; these are sensitive markers of the porphyrin core size, which are expanded in high-spin hemes, because an electron occupies the $d_{x^2-y^2}$ antibonding Fe orbital (*22*, *30*, *31*). The position of ν_{11} is at 1541 cm^{-1} (Figure 2C), a value confirmed via Q-band excitation (data not shown); there is no ν_{11} band in the His77Tyr variant near the 1529 cm^{-1} position found in the WT protein. We therefore conclude that replacement of His77 with tyrosine leads to (1) replacement of the strongly donating WT ligand with a moderate donor and (2) dissociation of one of the axial ligands in an appreciable fraction of the molecules, producing high-spin heme.

What is the nature of the strongly donating ligand in the WT protein? The Cys75 thiolate is an obvious candidate, since it is implicated by EPR as a ligand in the Fe(III) (*17*, *19*). However, thiolate binding to Fe(II) is precluded, since it would produce a Soret absorption band near 450 nm, as is observed for all low-spin Fe(II) adducts of cytochrome P450 (Table 2), in which the proximal ligand is thiolate. The Soret band for of Fe(II) CooA is at 424 nm, a typical value for nonthiolate heme complexes. The thiolate effect on the absorption spectrum is abolished if the thiolate becomes protonated, as is hypothesized to occur in cytochrome P420 or H450 (at low pH) (*32*, *33*). However, thiol is a neutral ligand and is not expected to perturb ν_{11}; it does not do so in the M80C cytochrome *c* mutant, in which cysteine replaces the Met80 ligand (Table 1) (*34*). Finally, ligation by Cys75 is ruled out by the observation that its replacement by serine or alanine has no effect on in vivo CO-dependent transcription (*19*).

Consequently, we infer that reduction of WT CooA is accompanied by a ligand switch from Cys75 to another

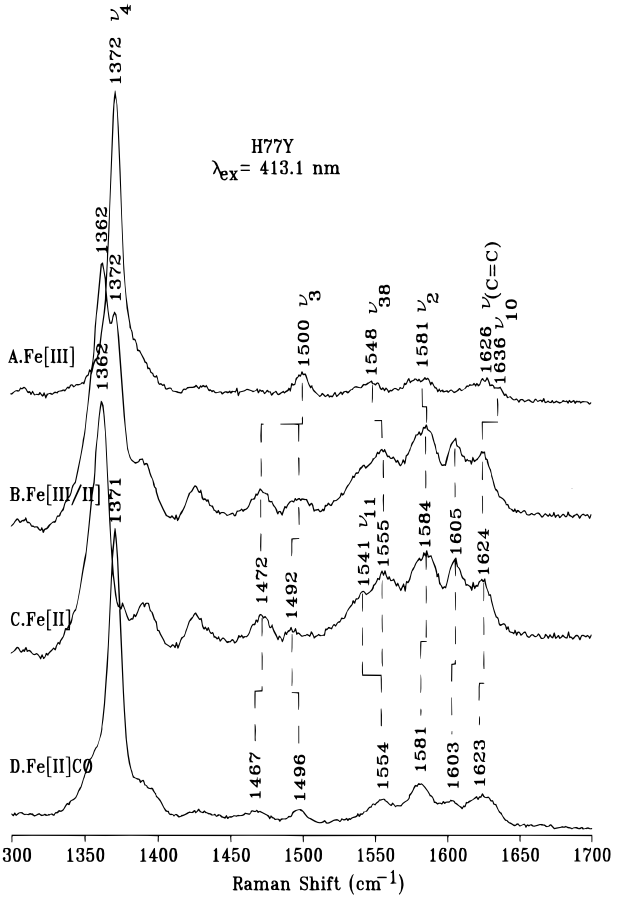

FIGURE 2: As in Figure 1 for the H77Y variant at 413.1 nm excitation. Due to the difficulty in producing a fully reduced Fe(II) adduct, we obtained the Fe(II) spectrum by subtracting trace A from trace B.

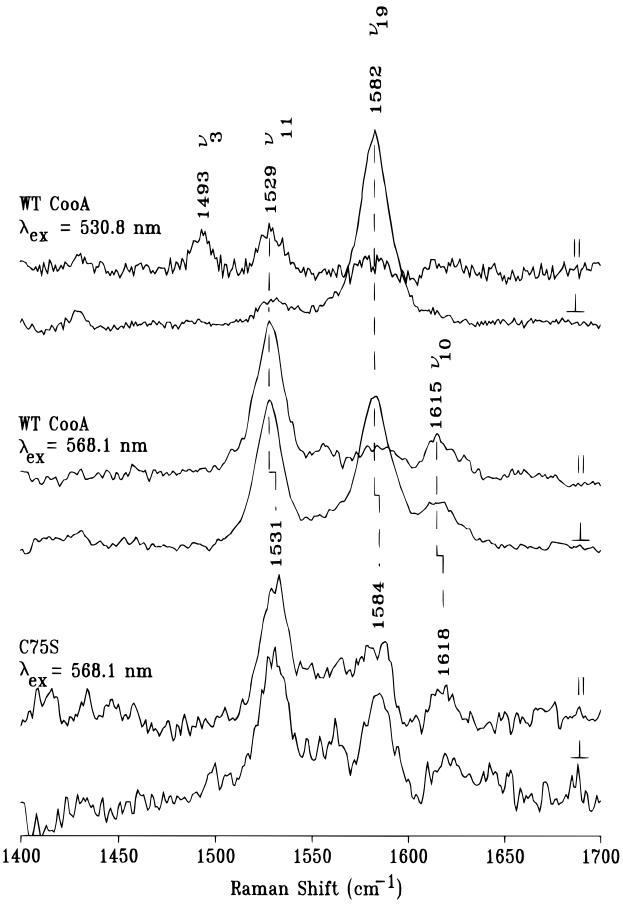

FIGURE 3: Q-band excited RR spectra of WT and Fe(II) CooA near resonance with the Q_1 (530.8 nm, top) and Q_o (568.1 nm, middle) electronic transitions and of the C75S variant with Q_o excitation (bottom). The spectra were obtained in parallel (||) and perpendicular (⊥) polarization.

residue with a strongly donating ligand. Because of its proximity and the dramatic effect of substitutions at this position, His77 is the obvious candidate. Replacement of histidine by tyrosine in H77Y CooA, a weak ligand for Fe(II), would explain the H77Y RR data. However, His77 cannot be a neutral imidazole ligand, because ν_{11} would then be at a position typical for PPIX(Im)$_2$, as it is in the H77Y mutant. The ν_{11} frequency, 1529 cm^{-1}, is consistent with imidazolate ligation (*27*, *28*). Since the pK_a of imidazole bound to Fe(II) heme is 13, an imidazolate ligand at neutral pH requires requires proton transfer to a protein acceptor in an environment protected from solvent (*28*).

There is precedent for imidazolate binding to Fe(II) heme in peroxidase enzymes, for which an aspartate side chain accepts a proton from the proximal histidine ligand (*35*). As a result, the 5-coordinate Fe(II)−N(His) stretching frequency is elevated to about the same value as in an imidazolate model complex (*36*). The identity of the proton acceptor in CooA is uncertain. Cys75 is an attractive candidate, since it is separated from His77 by only one intervening residue. Displacement of the thiolate ligand upon reduction of Fe(III) would be assisted by H-bond acceptance from His77, which would thereby acquire imidazolate character (Figure 4). However, Cys75 is not essential to CooA function, as shown by the activity assays for the Cys75Ser and Cys75Ala mutants (*19*). We examined Cys75Ser and found essentially the same RR spectra as the WT protein, including a depressed ν_{11} band in the Fe(II) form (Figure 3). Thus, imidazolate coordination is maintained in Fe(II) C75S, as it is in WT CooA. While the serine might substitute for cysteine as a proton acceptor for His77, a more likely scenario is that the proton acceptor is another proximal residue, Y, which is unaltered by mutation of Cys75.

CO-Bound Form. When CO is bound to either WT (Figure 1) or H77Y (Figure 2) CooA, the expected upshifts in ν_{11} and ν_4 are observed due to competition of the CO π^* orbitals with the porphyrin π^* orbitals for Fe d_π electrons (*25*). In addition, a small ν_3 component is detected at 1464 cm^{-1}, a high-spin position, indicating some steady-state 5-coordinate population due to CO photolysis. The ν_3 mode is known to be especially intense for high-spin heme and can be detected at quite low populations (*37*).

To examine the product of CO photolysis, we increased the laser flux substantially (Figure 5), shifting the majority of the ν_4 band intensity from the FeCO position, 1371 cm^{-1}, to the Fe(II) position, 1362 cm^{-1}. However, the 5-coordinate ν_3 intensity did not increase, and the spectrum remained characteristic of 6-coordinate low-spin heme; a ν_{11} shoulder reappeared at 1529 cm^{-1}, the WT Fe(II) CooA position. We conclude from this experiment that, although the bound CO is photolabile, recombination of the endogenous ligand displaced by the CO is rapid, so that the steady-state population under constant illumination is mainly the native 6-coordinate heme, not the 5-coordinate intermediate.

Table 2: Comparison of the Electronic Absorption Spectra of Fe(II) CooA with Heme Proteins and Model Complexes[a]

protein/model	ligands	δ (nm)	Soret (nm)	β (nm)	α (nm)	reference
WT CooA	?		426	529	559	this work
H77Y	?		419	530	557	*19*
C75S	?		423	527	557	*19*
cyt b_5	His/His		423	527	555	*55*
PPIX(ImH)(Im^-)	ImH/Im^-		433	532.5	563.5	*28*
MP8(ImH)(Im^-)	ImH/Im^-		422.5	525	553	*27*
cyt *c*	Met/His		416	520	550	*32*
P450 + THT	CysH/THT		422	530	560	*32*
cyt *c* (M80C)	CysH/His		416	520	550	*56*
H450, pH 6.0	CysH/His		425	530	560	*33*
P450 + *N*-phenylIm	Cys^-/Im		445	538	566	*32*
H450, pH 8.0	Cys^-/His		448	540	571	*33*
P450 + octanethiol	Cys^-/thiol		449	542	570	*32*
P450 + $(CH_3)_2S$	Cys^-/thioether	340/360	446	541	568	*32*

[a] Abbreviations: PPIX, protoporphyrin IX; MP8, microperoxidasae 8; THT, tetrahydrothiophene; py, pyridine.

In the low-frequency region (Figure 6), the CO adduct of WT CooA shows a prominent Fe−CO stretching band at 487 cm^{-1}, identifiable by its 4 cm^{-1} isotopic ^{13}CO shift. A weak δ(Fe−CO) band is also detected, at 572 cm^{-1}, and is quite apparent in the isotope difference spectrum, a frequency which has been observed in separate CooA samples. These frequencies are normal for heme−CO adducts having imidazole or other neutral proximal ligands (see below) (*38*, *39*). The ν(C−O) band is weak and is overlapped by overtone and combination bands of the porphyrin. The low signal strength reflects the fact that the C−O oscillator is only indirectly coupled to the porphyrin $\pi-\pi^*$ transitions, through the intervening Fe−CO bond (*40*). Consequently, resonant enhancement is low and is somewhat variable among different heme proteins. However, the interfering porphyrin bands are canceled in the isotope difference spectrum, leaving a clear sigmoidal difference band for ν(C−O), from which the frequency is reliably determined.

This frequency (which has been reproduced in separate CooA samples) is higher than in most heme proteins (*38*, *39*), and it differs significantly from the result reported recently by Uchida et al. (*16*). They found ν(Fe−CO) at the same frequency as we do, 487 cm^{-1}, but were unable to detect δ(Fe−CO), and their ν(C−O) was 1969 cm^{-1}. As pointed out by the authors, this ν(C−O) frequency and the absence of δ(Fe−CO) are characteristic of CO in a hydrophobic environment, but they are not the characteristics that we observe for WT CooA. Whether this variability is inherent in native CooA is uncertain. The differing RR spectra may reflect differences in the nature of the wild-type CooA samples analyzed. Our CooA samples are greater than 95% pure and have been shown to be active for CO-dependent DNA binding, while the purity and activity of the samples used by Uchida et al. (*16*) are undescribed.

Both WT CooA and the H77Y mutant give normal absorption spectra upon CO binding (419, 530, and 557 nm for the Soret, Q_1, and Q_0 bands, respectively (*6*)) but the RR spectra are distinctly different. For H77Y (Figure 7), *two* Fe−CO stretching bands are seen, 6 and 37 cm^{-1} above the Fe−CO frequency in WT CooA. The higher frequency, 524 cm^{-1}, is suggestive of a 5-coordinate CO adduct, in which the bond to the proximal ligand is broken (*38*, *39*, *41*). In the C−O stretching region, a single ^{13}CO sensitive band is observed, at 1969 cm^{-1}. Its intensity is higher than that of WT CooA, and we infer that it contains contributions from both the 5- and 6-coordinate adducts.

The correlation between ν(Fe−CO) and ν(C−O) (Figure 8) has become a useful tool for analyzing proximal and distal influences on the bound CO in heme adducts (*38*, *39*, *42*). For a given axial ligand, a negative linear correlation is found between ν(Fe−CO) and ν(C−O); the data points can range widely along this line due to back-bonding changes associated with electronic effects of porphyrin substituents or of the protein environment. The points for WT CooA and for the 6-coordinate adduct in the H77Y mutant fall on the correlation defined by the many heme proteins and models having neutral imidazole axial ligands, while the 5-coordinate H77Y adduct falls on a separate line defined by other 5-coordinate Fe(II) porphyrin adducts (*41*). Although the 6-coordinate H77Y and WT adducts fall on the same correlation, they do so at quite different points, indicative of different electronic environments.

The position of our CO adduct of WT CooA lies low on the back-bonding correlation, indicating a negative polar influence in the CO vicinity, which diminishes back-bonding to the CO. There is precedent for a negative protein environment in the myoglobin double mutant H64V/V68T, in which the distal histidine residue is replaced by the hydrophobic valine, while a nearby valine is replaced by the polar threonine (*43*). Crystallography reveals that the Thr68 OH group is H-bonded to the backbone carbonyl oxygen of the distal histidine so that its lone pair is oriented toward the bound CO, providing negative polarity (*44*, *45*). The resulting inhibition of back-bonding produces the anomalously high ν(C−O), 1984 cm^{-1}, and low ν(Fe−CO), 476 cm^{-1} (Figure 8).

The H77Y point is at essentially the same position as that of the A_0 substrate of CO-myoglobin (Mb), in which the distal histidine side chain has rotated out of the heme binding pocket, consequent to protonation, leaving the CO in a hydrophobic environment (*46*−*48*). The same position is seen for Mb mutants in which the distal histidine is replaced by residues with hydrophobic side chains (*43*, *49*). This is also the position of the CooA adduct reported by Uchida et al. (*16*). Our WT CooA point falls between this position and the H64V/V68T Mb position. Thus negative polarity is indicated, with about half the strength of the Thr OH lone pair in the Mb double mutant. A similar position is observed for the CO adduct of the M80C cytochrome *c* mutant, for which the lone pairs of the displaced neutral cysteine have been suggested to provide negative polarity to the bound CO (*34*).

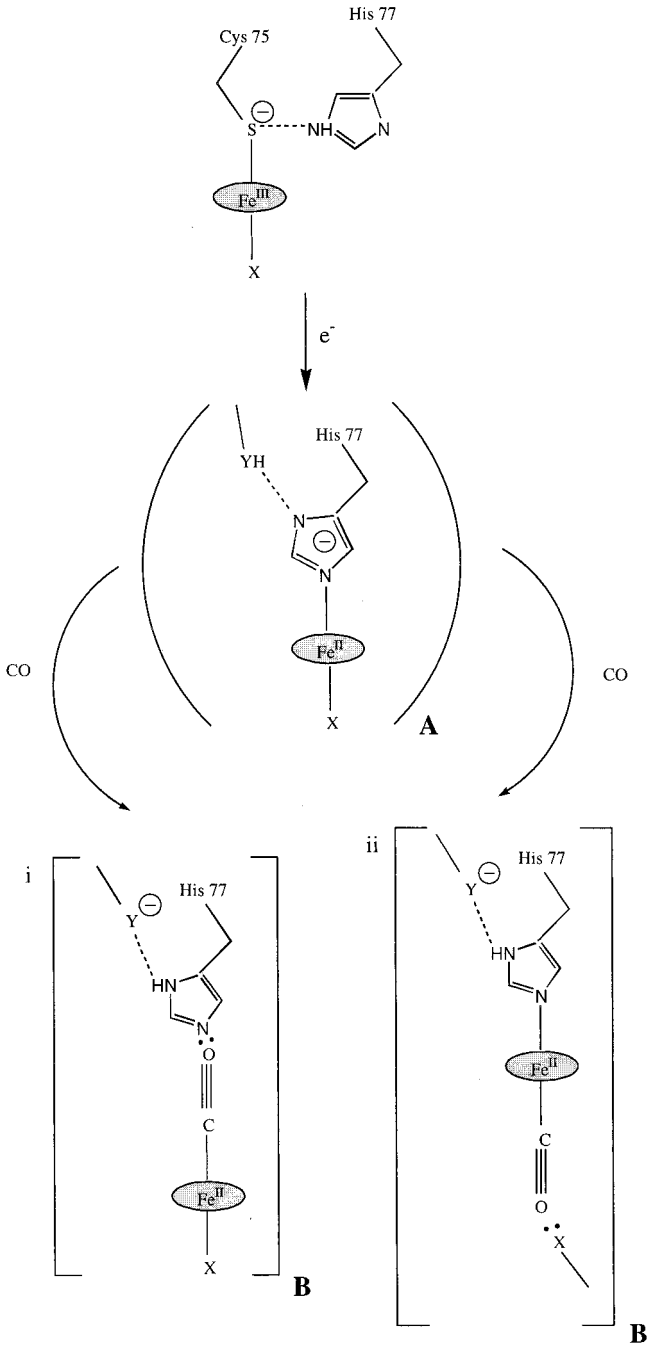

FIGURE 4: Models for CooA ligation changes during heme iron reduction and CO binding.

CO Adduct Models and Trans Ligand Effects. The identity of the trans ligand can also be investigated via the ν(Fe−CO)/ν(C−O) frequencies. The back-bonding correlation shifts to a lower position on the ν(Fe−CO) scale for imidazole complexes versus 5-coordinate CO adducts (Figure 8). This lowering results from competition between the imidazole and the CO for the Fe d_{z^2} σ-bonding orbital (*38*). A still lower correlation is found for the anionic ligands thiolate and imidazolate, because they are stronger donors than neutral imidazole. These electronic differences have been recently confirmed via density functional theory computations (*41*).

The effect on the back-bonding correlation of trans ligands other than imidazole and imidazolate or thiolate has not been evaluated. To gauge the likely effects of binding methionine

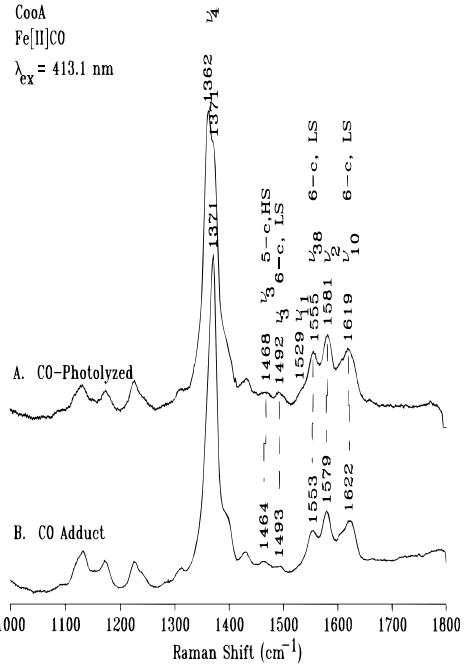

FIGURE 5: RR spectra in the porphyrin skeletal mode region for the CO adduct of WT CooA. Conditions: (A) sufficient power to partially photolyze the sample (120 mW power), focused beam, and spherical lens excitation; (B) under low power (50 mW), defocused beam, and cylindrical lens.

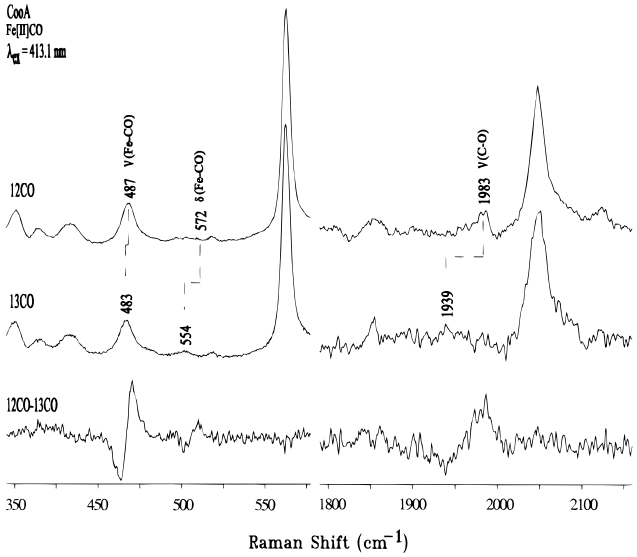

FIGURE 6: Isotope-edited RR spectra of the CO adducts of WT CooA, identifying the ν(Fe−CO) and ν(C−O) modes via $^{12/13}$C isotope shifts.

or un-ionized cysteine, we recorded RR spectra of CO adducts of Fe(II)OEP (OEP = octaethylporphyrin) and Fe(II) TPP (TPP = tetraphenylporphyrin) dissolved in the thioether solvents dibutyl sulfide (BS) and ethyl phenyl sulfide (EPS) (Figures 9 and 10). Significantly, the model data all fall on the same back-bonding correlation observed for the imidazole adducts (Figure 8). This means that ν(Fe−CO)/ν(C−O) data cannot be used to distinguish methionine from histidine coordination in proteins. From the point of view of the back-bonding correlation, thioethers have the same ligand donor strength as imidazole. To examine the effect of a neutral thiol, we also dissolved Fe(II)OEP in thiophenol and obtained a ν(Fe−CO) RR band at 496 cm^{-1} (data not shown).

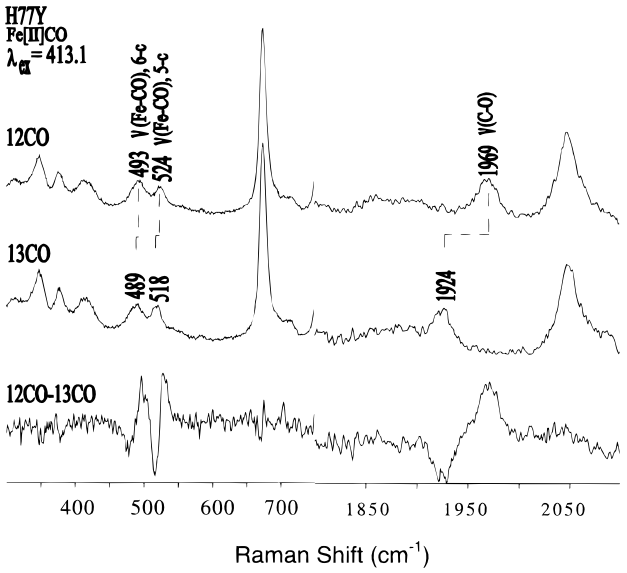

FIGURE 7: Isotope-edited RR spectra of the CO adducts of the H77Y variant, identifying the ν(Fe−CO) and ν(C−O) modes via $^{12/13}$C isotope shifts.

This is the same frequency as found for the *N*-methylimidazole complex of the Fe(II)OEP CO adduct (*50*, *51*). Unfortunately, we were unable to detect the ν(C−O) band, but it seems likely that CO adducts with neutral cysteine as axial ligand would also fall on the imidazole/thioether correlation.

Thus, the fact that WT CooA and also the H77Y mutant fall on the neutral ligand correlation means that the ligand trans to the CO could be histidine or methionine or neutral cysteine or another side chain of comparable donor strength, but it cannot be a strong donor such as ionized cysteine or imidazolate. This observation is consistent with CO displacing the imidazolate ligand leaving a neutral ligand, X, trans to the bound CO. If CO instead displaces X, then the bound imidazolate must be simultaneously reprotonated. In either case, the displaced ligand must remain in the binding pocket, with its lone pair oriented toward the bound CO, to explain the negative polarity which is evident in the back-bonding plot (Figure 4).

Further insight into the negative polarity can be gained from the thioether model compound data, which are spread out significantly on the back-bonding correlation (Figure 8). Part of the spread results from the greater electron withdrawing tendency of phenyl, relative to ethyl substituents on the porphyrin. The TPP points are lower on the back-bonding correlation, as has previously been observed for imidazole complexes (*38*, *39*). But there is also a difference between BS and EPS; for both OEP and TPP, the BS points fall lower on the back-bonding line than EPS, implying a different polarity of the CO environment. In these thioether solvents, the polar influence is mainly associated with the sulfur lone pairs, which are more extended in BS than EPS, since the phenyl group is electron withdrawing. Thus it is reasonable that the environmental polarity is more negative in BS than in EPS solvent, accounting for the diminished back-bonding.

DISCUSSION

Since CooA binds to a specific DNA sequence in a CO-dependent manner (*14*), it is likely that the act of CO binding

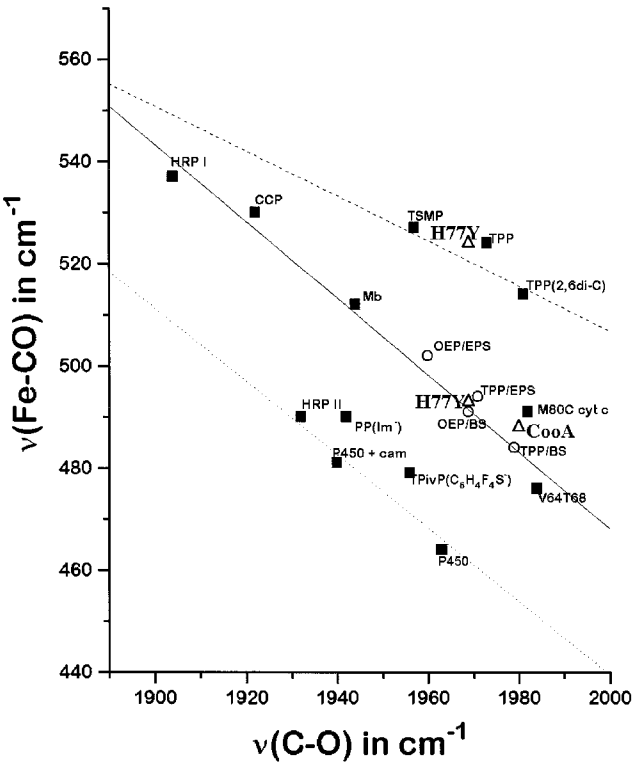

FIGURE 8: Plot of observed ν(Fe−CO) versus ν(C−O) frequencies for the CO adducts of WT CooA, H77Y, and select heme proteins and analogues. The solid line indicates the back-bonding correlation for proximal imidazole ligation; the dashed line is for 5-coordinate CO adducts; the dotted line is for thiolate and imidazolate ligation. Open triangles represent the CO adducts of wild-type and variant CooA; open circles represent heme(CO)(thioether) adducts. The remaining points (solid squares) represent 5-coordinate and 6-coordinate Fe(II)CO data taken from the larger data set reported by in refs *38*, *39*, and *41*. Labels: HRP, horseradish peroxidase; CCP, cytochrome *c* peroxidase; TSMP, tetrakis(*p*-sulfonatomesityl)-porphyrin; TPP, tetraphenylporphyrin; Mb, myoglobin; OEP, octaethylporphyrin; EPS, ethyl phenyl sulfide; BS, dibutyl sulfide; cyt *c*, cytochrome *c*; P450, cytochrome P450; cam, camphor; Im^-, imidazolate; TPivP, picket fence porphyrin.

triggers a conformation change that positions the helix−turn−helix in the proper orientation for sequence-specific DNA binding (*16*). The native protein contains low-spin heme and therefore must supply two endogenous ligands, on either side of the heme plane, to achieve a large enough ligand field. Since the CO also binds the heme, it follows that at least one of the ligands must be displaced. It is reasonable to expect that this displacement provides the trigger for the required conformational change. Therefore, identifying the endogenous heme ligands is a prerequisite for understanding the activation mechanism.

Recent work by Shelver et al. (*19*) utilized extensive site-directed mutagenesis, electronic absorption and EPR spectroscopies, and biochemical analysis of Cys75 and His77 variants in the oxidized, reduced, and CO-bound forms. This work suggested that Cys75 is a heme ligand in the Fe(III) form and His77 is a ligand in the Fe(II) form, but the assignment of the latter was indirect. The present work establishes that the His77 ligand is deprotonated, implying the presence of a proton acceptor, Y (Figure 4), analogous to the proximal aspartate residue in peroxidases (*35*).

However, the Fe−CO frequencies also establish that when CO binds to CooA, the adduct has a neutral trans ligand,

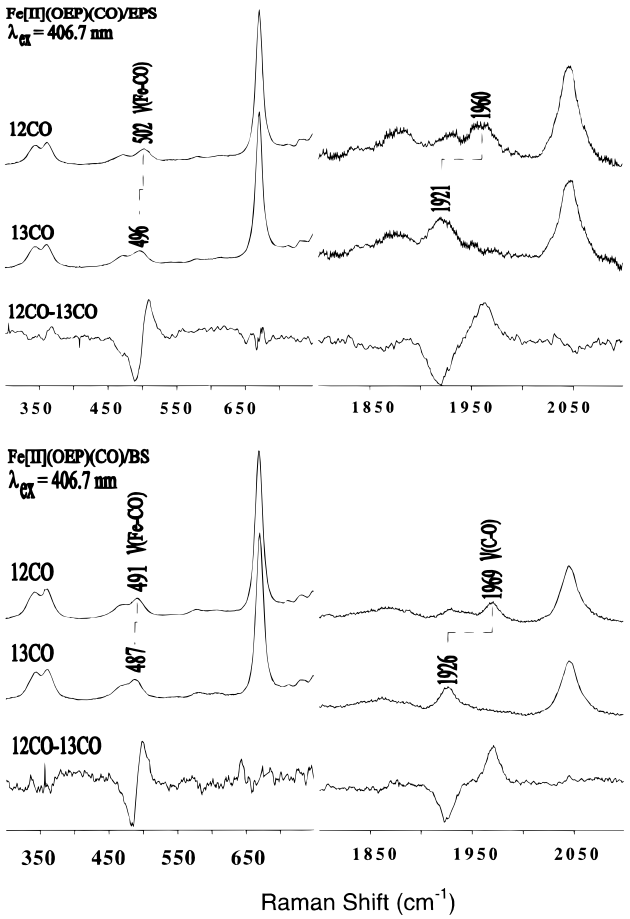

FIGURE 9: Isotope-edited RR spectra of the CO adducts of Fe(II)-OEP in dibutyl sulfide (BS) and ethyl phenyl sulfide (EPS), identifying the ν(Fe−CO) and ν(C−O) modes via $^{12/13}$C isotope shifts.

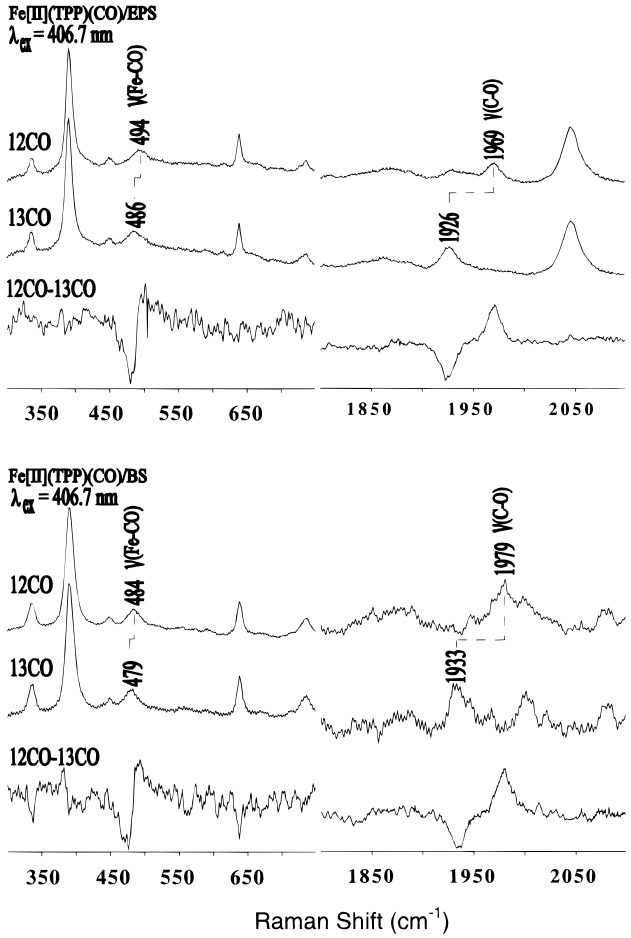

FIGURE 10: As in Figure 8, for Fe(II)TPP, with 406.7 nm excitation.

instead of imidazolate. There are two possibilities to explain this observation: (i) CO displaces His77 leaving X bound to the iron (in that case X must be a neutral ligand) or (ii) CO displaces X leaving His77 bound to the iron (in that case His77 must simultaneously be reprotonated, thereby becoming a neutral ligand).

Let us consider the implications of these two scenarios for the mechanism of CooA activation. There must be two states, A and B, of the protein, having low and high affinity for sequence-specific binding of DNA. CO binding induces the change from A to B. In scenario i displacement of His77 raises the pK_a of the imidazolate ligand because its charge is no longer stabilized by the Fe(II). This will induce reprotonation from the adjacent YH, producing a charge relay YH- - -His$^-$ → Y$^-$- - -HisH. This charge relay would have two functions: (a) It would facilitate CO binding, by stabilizing the displaced protein ligand. Ordinarily, CO does not compete effectively with endogenous ligands in heme proteins. When the ligand is tethered to the polypeptide chain, its displacement from the iron has a high-energy barrier. The charge relay would lower the barrier by replacing the departing ligand with a proton. (b) The developing negative charge on Y$^-$ could induce the A → B conformational change by attracting positive charges or dipoles; the polypeptide motion caused by the His77 displacement could also aid this transition. Thus scenario i provides a straightforward explanation for facilitating CO binding and coupling this event to a specific conformational change of the protein via the displacement of charge from His$^-$ to Y$^-$.

In scenario ii the protein conformational change could still be induced by the charge relay. Reprotonation of His77 upon CO displacement of X would explain the presence of a neutral ligand, trans to the bound CO. In this case, however, the trigger for the conformational change would be the polypeptide motion associated with the displacement of X.

If we accept that the A → B conformational change is induced by the HY- - -His$^-$ → Y$^-$- - -HisH charge relay, then the choice of scenario i or ii depends on which bond, the Fe−His or Fe−X, is displaced by CO once the charge is transferred. The charge relay provides a simple electronic explanation for Fe−His$^-$ lability, but it cannot be excluded that the protein forces are arranged to favor Fe−X displacement. Further experiments are required to determine which bond is displaced.

Likewise, further experiments are required to determine the identity of the proton acceptor, Y$^-$. The thiolate side chain of Cys75 is an appealing candidate since it is a ligand in the Fe(III) form and probably accepts a H-bond from His77 (Figure 4). Proton transfer to Cys75 would be a natural accompaniment to the Cys75/His77 ligand switch. However, the mutational evidence is that Cys75 can be replaced by serine or alanine with no effect on in vivo activity. Consequently, another residue instead of, or in addition to, Cys75 seems to function as a proton acceptor.

In conclusion, the spectroscopic and mutational data on CooA provide strong evidence for a novel redox-induced

ligation switch between the nearby cysteine and histidine residues. The switch to histidine is accompanied by a proton transfer to a nearby acceptor. CO binding induces a charge relay resulting in reprotonation of His77 which induces the proton conformational change which is required for sequence-specific DNA binding. The charge relay and conformation change are an electronic consequence of ligand displacement, either of His77 or of the trans ligand, X, by the CO.

ACKNOWLEDGMENT

We acknowledge Drs. Robert L. Kerby and Robert Williams for critical reading and help with the manuscript and Ms. Christina Zeigler for technical assistance.

REFERENCES

1. Ignarro, L. J., Degnan, J. N., Baricos, W. H., Kadowitz, P. J., and Wolin, M. S. (1982) *Biochim. Biophys. Acta 718*, 49−59.
2. Craven, P. A., and DeRubertis, F. R. (1983) *Biochim. Biophys. Acta 745*, 310−321.
3. Ignarro, L. J. (1989) *Semin. Hematol. 26*, 63−76.
4. Gilles-Gonzalez, M. A., Gonzalez, G., and Perutz, M. P. (1995) *Biochemistry 34*, 232−236.
5. Gilles-Gonzalez, M. A., Ditta, G. S., and Helinski, D. R. (1991) *Nature 350*, 170−172.
6. Shelver, D., Kerby, R. L., and Roberts, G. P. (1997) *Proc. Natl. Acad. Sci. U.S.A. 94*, 11216−11220.
7. Deinum, G., Stone, J. R., Babcock, G. T., and Marletta, M. A. (1996) *Biochemistry 35*, 1540−1547.
8. Yu, A. E., Hu, S., Spiro, T. G., and Burstyn, J. N. (1994) *J. Am. Chem. Soc. 116*, 4117−4118.
9. Tomita, T., Ogura, T., Tsuyama, S., Imai, Y., and Kitagawa, T. (1997) *Biochemistry 36*, 10155−10160.
10. Burstyn, J. N., Yu, A. E., Dierks, E. A., Hawkins, B. K., and Dawson, J. H. (1995) *Biochemistry 34*, 5896−5903.
11. Stone, J. R., Sands, R. H., Dunham, W. R., and Marletta, M. A. (1995) *Biochem. Biophys. Res. Commun. 207*, 572−577.
12. Kerby, R. L., Hong, S. S., Ensign, S. A., Coppoc, L. J., Ludden, P. W., and Roberts, G. P. (1992) *J. Bacteriol. 174*, 5284−5294.
13. Kerby, R. L., Ludden, P. W., and Roberts, G. P. (1995) *J. Bacteriol. 177*, 2241−2244.
14. He, Y., Shelver, D., Kerby, R. L., and Roberts, G. P. (1996) *J. Biol. Chem. 271*, 120−123.
15. Kolb, A., Busby, S., Buc, H., Garges, S., and Adhya, S. (1993) *Annu. Rev. Biochem. 62*, 749−795.
16. Uchida, T., Ishikawa, H., Takahashi, S., Ishimori, K., Morishima, I., Ohkubo, K., Nakajima, H., and Aono, S. (1998) *J. Biol. Chem. 273*, 19988−19992.
17. Reynolds, M. F., Shelver, D., Kerby, R. L., Parks, R. B., Roberts, G. P., and Burstyn, J. N. (1998) *J. Am. Chem. Soc. 120*, 9080−9081.
18. Aono, S., Nakajima, H., Saito, K., and Okada, M. (1996) *Biochem. Biophys. Res. Commun. 228*, 752−756.
19. Shelver, D., Thorsteinsson, M. V., Kerby, R. L., Chung, S.-Y., Roberts, G. P., Reynolds, M. F., Parks, R. B., and Burstyn, J. N. (1999) *Biochemistry 38*, 2669−2678.
20. de Duve, C. (1948) *Acta Chem. Scand. 2*, 264−289.
21. Tsai, A.-L., Kulmacz, J.-S. W., Wang, Y., Van Wart, H. E., and Palmer, G. (1993) *J. Biol. Chem. 268*, 8554−8563.
22. Spiro, T. G., and Strekas, T. C. (1974) *J. Am. Chem. Soc. 96*, 338−345.
23. Hu, S., Smith, K. M., and Spiro, T. G. (1996) *J. Am. Chem. Soc. 118*, 12638−12646.
24. Anzenbacher, P., Evangelista-Kirkup, R., Schenkman, J., and Spiro, T. G. (1989) *Inorg. Chem. 28*, 4491−4495.
25. Choi, S., Spiro, T. G., Langry, K. C., Smith, K. M., Budd, D. L., and Mar, G. N. L. (1982) *J. Am. Chem. Soc. 104*, 4345−4351.
26. Cartling, B., and Wilbrandt, R. (1981) *Biochim. Biophys. Acta 637*, 61−68.
27. Othman, S., Lirzin, A. L., and Desbois, A. (1994) *Biochemistry 33*, 15437−15448.
28. Desbois, A., and Lutz, M. (1992) *Eur. Biophys. J. 20*, 321−335.
29. Spiro, T. G., and Strekas, T. C. (1972) *Proc. Natl. Acad. Sci. U.S.A. 69*, 2622−2626.
30. Spiro, T. G., Ed. (1988) *Biological Applications of Raman Spectroscopy*, Vol. 3, John Wiley & Sons, Inc., New York.
31. Kitagawa, T., Kyogoku, Y., Iizuka, T., Ikeda-Saito, M., and Yamanaka, T. (1974) *J. Biol. Chem. 78*, 719−728.
32. Dawson, J. H., Andersson, L. A., and Sono, M. (1983) *J. Biol. Chem. 258*, 13637−13645.
33. Omura, T., Sadano, H., Hasegawa, T., Yoshida, Y., and Kominami, S. (1984) *J. Biochem. 96*, 1491−1500.
34. Smulevich, G., Bjerrum, M. J., Gray, H. B., and Spiro, T. G. (1994) *Inorg. Chem. 33*, 4629−4634.
35. Mincey, T., and Traylor, T. G. (1979) *J. Am. Chem. Soc. 101*, 765−766.
36. Stein, P., Mitchell, M., and Spiro, T. G. (1980) *J. Am. Chem. Soc. 102*, 7795−7797.
37. Smulevich, G., Miller, M. A., Gosztola, D., and Spiro, T. G. (1989) *Biochemistry 28*, 9905−9908.
38. Li, X.-Y., and Spiro, T. G. (1988) *J. Am. Chem. Soc. 110*, 6024−6033.
39. Ray, G. B., Li, X.-Y., Ibers, J. A., Sessler, J. L., and Spiro, T. G. (1994) *J. Am. Chem. Soc. 116*, 162−176.
40. Jewsbury, P., Yamamoto, S., Minato, T., Saito, M., and Kitagawa, T. (1995) *J. Phys. Chem. 99*, 12677.
41. Vogel, K. M., Kozlowski, P., Zgierski, M. Z., and Spiro, T. G. (1999) *Inorg. Chim. Acta* (submitted for publication).
42. Kerr, E. A., and Yu, N.-T. (1988) in *Biological Applications of Raman Spectroscopy* (Spiro, T. G., Ed.) Vol. 3, pp 39−96, John Wiley & Sons, Inc., New York.
43. Li, T., Quillin, M. L., George N. Phillips, J., and Olson, J. S. (1994) *Biochemistry 33*, 1433−1446.
44. Smerdon, S. J., Dodson, G. G., Wilkinson, A. J., Gibson, Q. H., Blackmore, R. S., Carver, T. E., and Olson, J. S. (1991) *Biochemistry 30*, 6252−6260.
45. Cameron, A. D., Smerdon, S. J., Wilkinson, A. J., Habash, J., Helliwell, J. R., Li, T., and Olson, J. S. (1993) *Biochemistry 32*, 13061−13070.
46. Han, S., Rousseau, D. L., Giacometti, G., and Brunori, M. (1990) *Proc. Natl. Acad. Sci. U.S.A. 87*, 205−209.
47. Ramsden, J., and Spiro, T. G. (1989) *Biochemistry 28*, 3125−3128.
48. Fuchsman, W. H., and Appleby, C. A. (1979) *Biochemistry 18*, 1309−1321.
49. Morikis, D., Champion, P. M., Springer, B. A., and Sligar, S. G. (1989) *Biochemistry 28*, 4791−4800.
50. Kerr, E. A., Mackin, H. C., and Yu, N.-T. (1983) *Biochemistry 22*, 4373−4379.
51. Hashimoto, T., Dyer, R. L., Crossley, M. J., Baldwin, J. E., and Basolo, F. (1982) *J. Am. Chem. Soc. 104*, 2101−2109.
52. Li, X.-Y., Czernuszewicz, R. S., Kincaid, J. R., Stein, P., and Spiro, T. G. (1990) *J. Chem. Phys. 1990*, 47−61.
53. Desbois, A., Tegoni, M., Gervais, M., and Lutz, M. (1989) *Biochemistry 28*, 8011−8022.
54. Hu, S., Morris, I. K., Singh, J. P., Smith, K. M., and Spiro, T. G. (1993) *J. Am. Chem. Soc. 115*, 12446−12458.
55. Beck von Bodman, S., Schuller, M. A., Jollie, D. R., and Sligar, S. G. (1986) *Proc. Natl. Acad. Sci. U.S.A. 83*, 9443−9447.
56. Raphael, A. L., and Gray, H. B. (1991) *J. Am. Chem. Soc. 113*, 1038−1040.

BI982375R